Spectral line shape of the $P(2)$ transition in CO-Ar: Uncorrelated *ab initio* calculation

R. Wehr,[1] A. Vitcu,[1] R. Ciuryło,[2] F. Thibault,[3] J. R. Drummond,[1] and A. D. May[1,*]
[1]*Department of Physics, University of Toronto, Toronto, Ontario, Canada, M5S 1A7*
[2]*Institute of Physics, Nicholas Copernicus University, Grudziądzka 5/7, 87-100 Toruń, Poland*
[3]*UMR 6627 du CNRS, Université de Rennes, Campus de Beaulieu, 34042 Rennes Cedex, France*
(Received 17 June 2002; published 12 December 2002)

We calculate the spectral line shape of an isolated line from first principles, assuming that the translational motion is not statistically correlated with the evolution of the optical coherence, i.e., with the broadening. We use the known, realistic potentials for the influence of collisions on the translational motion and on the internal motion. We show that the calculated profiles do not agree, particularly at low pressures, with very precise experimental profiles of the $P(2)$ line of CO in a bath of Ar. We establish that the source of the disagreement lies in the assumption of uncorrelated effects of collisions on the translational motion and the optical coherence associated with the internal degrees of freedom.

DOI: 10.1103/PhysRevA.66.062502 PACS number(s): 32.70.Jz

I. INTRODUCTION

As recently stressed [1], the shape of a spectral line is obtained by solving a master transport/relaxation equation for the off-diagonal element of the density matrix. In principle, a solution of the full (tensorial) transport/relaxation equation will yield not only the width and shift of lines but also the line shape, starting only from the interaction potential between the active molecule and its perturbers. Such *ab initio* line shapes are expected to differ from all of the standard line shapes, such as Lorentz, Voigt, Galatry, speed-dependent Voigt, etc. (see Refs. [1–5], and references therein). To date, there has been (to the best of our knowledge) only a single calculation of this nature [6]. There, a ''restricted form'' of the master equation was used, and the main thrust of the paper was to compare between a number of model solutions of the master equation. The case considered was for the Raman Q branch of D_2 in a bath of He and the main point of the comparison with experiment was to demonstrate that the *ab initio* calculation showed the Dicke narrowing of the lines at low density. We are interested in obtaining the line shape at all densities and pressures.

Two approximations (beyond the usual binary-collision impact approximation) were made in Ref. [1]. The first one was a scalar as opposed to a tensorial formulation of the master equation, and the second was a restriction, in general, to the situation where the effects of collisions on the internal degrees of freedom are uncorrelated with the effects of collisions on the translational motion. A general formalism for solving this scalar transport/relaxation equation, with or without statistical correlation, was recently presented [7]. In fact, this is a simplified version of an approach given earlier by Blackmore [8]. Hereafter, we refer to Ref. [7] as part I. In Ref. [9] we explored, for the uncorrelated case, the influence of the ratio of the mass of the perturber to the mass of the active molecule, the ratio of the optical to kinetic cross section and the density, on theoretical spectral profiles. For the uncorrelated case, there is no technical difficulty in taking different potentials to determine the translational motion and the relaxation of the optical coherence (broadening and shifting) [8]. In Ref. [9] the potential controlling the translational motion was taken as that for rigid spheres whereas, in essence, the potential controlling the broadening, $\Gamma(v)$, and the shifting, $\Delta(v)$, was assumed to be of a form that yielded relaxation rates approximately quadratic in the speed v, of the active molecule. Hereafter, we refer to Ref. [9] as part II.

The present paper is very much a continuation of parts I and II. Here we have in mind a comparison of *ab initio* calculations with experimental results for the CO-Ar system. In contrast to part II where a form of $\Gamma(v)$ was assumed, we choose instead an established CO-Ar potential-energy surface (PES) to calculate the speed dependence of the broadening. As is appropriate for CO-Ar, we continue to set the shift equal to zero. CO-Ar was chosen not only because the PES is known, but also because we have available the experimental data for the very precise measurements of Berman *et al.* [10] of the $P(2)$ and $P(7)$ lines at 301 K. We restrict the calculation to the $P(2)$ line, a line that has yielded widely varying values of the velocity relaxation rate (narrowing parameter) when fitted with different spectral models (see Fig. 4 in Ref. [4] and compare correlated and uncorrelated models). Details of the difference frequency spectrometer used to make the measurements were given in Ref. [10] and references therein.

The master equation, like the closely related Boltzmann equation, is a complicated integral-differential equation. The usual method of solving such equations is to expand the solutions in terms of a complete orthonormal set of functions in velocity space. This converts the problem to a set of coupled linear equations involving ''matrix elements'' (weighted integrals over velocity) of various terms in the transport/relaxation equation. This formalism was laid out in part I and will not be repeated. Here, the only calculational difference from part II (aside from choosing input parameters appropriate to CO-Ar) is, as stated above, that instead of assuming a form for $\Gamma(v)$, we calculate it from a PES.

II. CALCULATED SPEED-DEPENDENT BROADENING

Fully quantal close-coupled calculations of the broadening coefficient were carried out using the PES of

*Author to whom all correspondence should be addressed. Email address: dmay@physics.utoronto.ca

Toczyłowski and Cybulski [11]. It is fortunate that the speed dependence of the relaxation of the optical coherence makes its presence felt more in the shape of the line (non-Lorentzian, for example) rather than in the overall width of the line. One may then test the quality of a potential by comparing a thermally averaged broadening coefficient with an experimental value obtained by fitting (high-density) data to a Lorentzian line shape. In Ref. [12] it was shown that the Toczyłowski and Cybulski [11] potential yielded broadening coefficients (when *evaluated at a mean relative speed*) that were in close agreement with experimental results. More recently, it has been shown [13] that *thermally averaged* broadening coefficients are in better agreement with the most precise experimental data. The accuracy ($\pm 2\%$ or better) is perhaps the best one can expect, given that the calculation ignores the influence of the speed of the active molecule on the line shape. In this paper, we are primarily interested in the speed dependence of the broadening and its influence on the shape of the line.

Details of the close-coupled calculations of the broadening, $\Gamma(v_{\rm rel})$, as a function of the relative speed, $v_{\rm rel}$, have been given elsewhere (Refs. [12,13], and references therein); and once again, in the interest of brevity, will not be repeated here. They were carried out at the Université de Rennes using both the MOLSCAT [14] and the MOLCOL codes [15]. Figure 1(a) shows, for the $P(2)$ line of CO highly diluted in Ar, a plot of the cross section $\sigma(E)$ as a function of the kinetic energy $E=\mu v_{\rm rel}^2/2$, where μ is the reduced mass of the CO-Ar system, $v_{\rm rel}$ is the relative speed $|\vec{v}-\vec{v}_p|$, and $\vec{v}_p$ is the perturber velocity. Figure 1(b) shows that the numerical values of $\sigma(E)$ are well fitted by a straight line on a log/log plot. We find the cross section is well represented analytically by $\sigma(E)=\sigma_0(E/E_0)^q$; with $\sigma_0=361(6)$ Å, $E_0=1$ cm^{-1}, and $q=-0.250(3)$. [Here and below, (x) signifies the uncertainty (standard deviation) in the last significant figure reported. In the fitting routine we ignored the points below 10 cm^{-1}.] It follows that the broadening coefficient has the form $\Gamma(v_{\rm rel})=Av_{\rm rel}^n$, where A is a constant and $n=1+2q$. The speed-dependent broadening coefficient to be used in the transport/relaxation equation for the off-diagonal element of the density matrix is a thermal average of $\Gamma(v_{\rm rel})$ over $\vec{v}_p$, with $\vec{v}$ held constant. Using the fitted curve for $\Gamma(v_{\rm rel})$, the conversion from $\Gamma(v_{\rm rel})$ to $\Gamma(v)$ can be carried out analytically. The result is, $\Gamma(v)=\Gamma_0(1+\alpha)^{-n/2}M(-n/2,3/2,-\alpha v^2/v_m^2)$, (Ref. [3]), where v is the speed of the active molecule CO, $v_m=\sqrt{2k_BT/m}$ is the most probable speed of the active molecule, $\alpha=1.4829$ is the ratio of the mass of Ar to that of CO, n equals $[(1-2)\times 0.250(3)=0.500(6)]$, and $M(a,b,z)$ is the confluent hypergeometric function. The thermally averaged value of $\Gamma(v)$ equals Γ_0 and its calculated value for the $P(2)$ line is 64.55×10^{-3} cm^{-1}/atm [13]. In Fig. 1(c), we show a plot of $\Gamma(v)$ and the Maxwell speed distribution as a function of v/v_m. We see that Γ varies significantly over the range $[(0-2)v_m]$. Having an analytical expression for $\Gamma(v)$ is very convenient for the numerical evaluation of the line shape. The irregularities in Figs. 1(a) and 1(b), at low energy, are not due to uncertainties in the calculations but rather arise from resonances in the cross section. Thermal averaging over the motion of the perturber will smoothen these out, and consequently, we believe that $\Gamma(v)$ [derived from a *smooth fit* to $\sigma(E)$], is accurate.

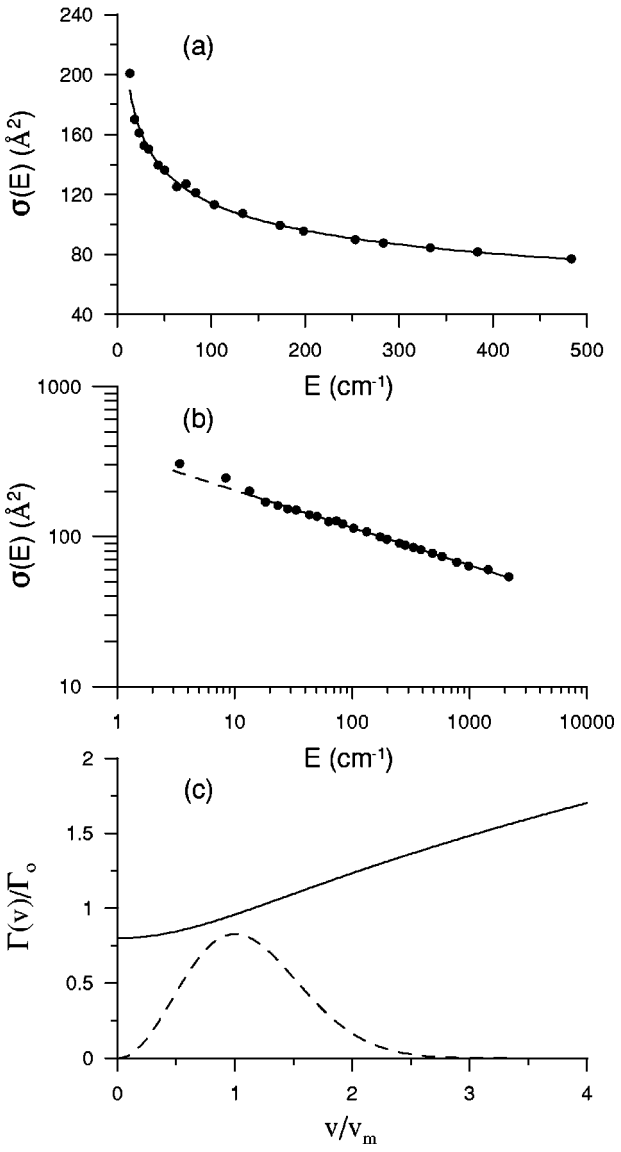

FIG. 1. (a) A linear and (b) logarithmic plot of the calculated cross section for the broadening of the $P(2)$ line in CO-Ar at 301 K, as a function of the relative kinetic energy. (c) The calculated "width" of the $P(2)$ line as a function of the speed of the CO molecule. Included, as a dashed line, is a plot of the Maxwell distribution function for CO.

III. COMPUTATION AND COMPARISON

As given in part II, and repeated here for clarity, the line shape $I(\omega)$ is given by $I(\omega)=\mathrm{Re}\ c_0(\omega)/\pi$, where c_0 is obtained by solving the complex set of linear equations, $\underline{\mathbf{b}}=\mathbf{L}(\omega)\underline{\mathbf{c}}(\omega)$, where $\underline{\mathbf{c}}(\omega)$ and $\underline{\mathbf{b}}$ are single-column matrices. The basis functions $\varphi_s(v)$, used to calculate the "matrix elements" are labeled with a subscript s $(s=0,1,\ldots)$ and chosen such that $\varphi_0(v)=1$. With this convention, the ele-

ments of $\underline{\mathbf{b}}$ are given by $[\underline{\mathbf{b}}]_s = \delta_{s,0}$. The matrix $\mathbf{L}(\omega)$ is given by $\mathbf{L}(\omega) = -i(\omega - \omega_0)\mathbf{1} + i\mathbf{K} - \mathbf{S}_D^f - \mathbf{S}_{VC}^f$, where ω_0 is the free molecule resonant frequency, $\mathbf{K}$ is the Doppler-shift matrix, and the $\mathbf{S}$'s are matrices arising from the broadening (dephasing) and velocity changing collision operators. The basis functions used here are the same as those used in part II. An expression [Eq. (9)] for the elements of $\mathbf{K}$ was given in Part II along with expressions allowing one to calculate the elements of $\mathbf{S}_{VC}^f$ for the case of interacting rigid spheres [16,17]. For this part of the problem one needs both masses and the mean collision diameter. To fix the latter, we equate the calculated diffusion constant [see Eqs. (16) and (19) in part II] to the measured mass diffusion constant [18]. We use our analytical expression for $\Gamma(v)$ (given above) and Eq. (11) of part II to calculate $\mathbf{S}_D^f$, i.e., to calculate the matrix elements of $\Gamma(v)$. Thus all of the elements of L can be calculated and a numerical solution of the coupled linear equations determined. Of course, there is always a question of selecting the number of basis functions to be included. Here we simply started with low values of s and increased it until the resulting spectrum appeared to have converged to less than the noise in the experimental results. We come back to this question below.

While the calculation of the line shape starting from an interaction potential is an *ab initio* calculation, a comparison of the calculated, normalized, absorption profiles, $I_c(\omega_i)$, with the measured absorption profiles, $I_m(\omega_i)$, still requires the use of fitting parameters. [By $I_m(\omega)$ we mean $-\ln(R(\omega))$, where $R(\omega)$ is the ratio of the intensity transmitted by the gas cell to the intensity of the reference beam.] The fitting parameters warrant detailed discussion. The line strength, the density of CO, and length of cell used in Ref. [10] are not known well enough, so that we can assign them a value for the computed line shape. Thus we treat S, the ''area'' under the calculated absorption curve, as an adjustable parameter. Variation or uncertainty in the measured base line impacts on the measured absorption profile. Even though the experimental base line reported in Ref. [10] was flat to within 1 part in 800, we still allowed it to ''float'' in the fitting routine. In practice, we do not match the calculated and experimental integrated line intensity, but rather our program varies S and BL to minimize $\Sigma_i[SI_c(\omega_i) - I_m(\omega_i) + \ln(\mathrm{BL})]^2$, where the sum is over all points i, and BL stands for base line. We allow BL to vary linearly with frequency across the line. If the calculated and measured profiles are the same, our fitting routine will yield identical integrated intensities.

While the calculated broadening coefficient is probably reliable to better than 2%, widths determined by fitting to the data of Ref. [10] are accurate to about 0.1%. Since we are interested in the influence of the speed dependence of Γ on the *shape* of the line, and since the influence is known to be weak, we are probably safe in assuming that the PES is known well enough that we can trust the calculated variation of Γ with speed and the only significant uncertainty in the calculation of Γ is the value of Γ_0. The fitting routine used considers Γ_0 as a third adjustable parameter.

Finally, there are two other minor fitting parameters. The experiments [10] did not include an absolute measurement of the line positions. Consequently, the position of line center was also allowed to float. Furthermore, experimental results for CO-N_2 [19] and CO-Ar [10] have revealed the presence of weak line mixing in the CO system at the pressures used in the experiments. Usually, for a comparison of the calculated and measured profiles, the effect of mixing would be removed from the experimental data by decomposing it into a symmetric and an asymmetric component, a form well known for weak mixing [20]. Here, for technical reasons, we add a mixing term to the calculated profile. The set of linear equations [see above or Eq. (2) in part II] are written such that mixing can be incorporated by multiplying $\underline{\mathbf{b}}$ by $(1 - iY)$, where Y is the weak mixing parameter. Thus in the actual fitting routine $I_c(\omega_i)$ is replaced by $I_c^y(\omega_i)$, indicating the inclusion of weak line mixing. In summary, the adjustable parameters in the fitting routine were (i) S, the overall amplitude, (ii) the base line BL, (iii) Γ_0, the overall width, (iv) ω_0, the central frequency, and (v) Y, the weak mixing parameter. In principle, except for Γ_0, these do not influence the *shape* of the symmetric component. Varying Γ_0 by a few percent acts like a scaling factor for the frequency scale (at least at high pressures) but does not alter the intrinsic shape of the calculated line. The shape is dominated by the fact that we have chosen an uncorrelated model for the transport/relaxation equation and the calculated speed dependence of the broadening coefficient. It is known [21,22] for the translational motion alone, i.e., no broadening, that the spectral line shape is insensitive to the form of the potential, provided the potential is chosen to yield the same high-density result, i.e., to yield the same diffusion constant. Thus the *shape* would not be expected to change significantly if we were to model the translational motion using, say, a Lennard-Jones potential as opposed to a rigid sphere.

We are now in a position to compare the *shapes* of the computed and measured profiles for the $P(2)$ line of CO highly diluted in Ar. In Ref. [10], results were given at nine pressures from 0.05 to 0.99 atm. Each dataset contained some 125 discrete measurements with fewer points recorded in the wings than in the core of the line. We compare the shapes in two ways, directly and as the difference between the two. In the upper panel of Figs. 2(a)–2(d), we show plots, at four pressures, of the computed profile superimposed on the experimental points. In the terminology of part II, convergence of the calculated curves to within the experimental noise was achieved at the lowest pressure by including basis functions with n and l up to 10 (121 basis functions). At the highest pressure, n and l up to 5 (36 basis functions) was sufficient to achieve convergence. On the scale of the figure, the shape of the computed curve appears to agree with the measured line shape at all pressures. However, on an expanded scale there are significant differences. In the second panel of Figs. 2(a)–2(d) we show a plot of 100 times the residuals or difference between the data and the calculated spectrum at the same frequency, $[S_{\mathrm{fit}} I_c^y(\omega_i)_{\mathrm{fit}} - I_m(\omega_i) + \ln(BL_{\mathrm{fit}})]$, joined together by straight line sections. It is clear from the second panels that the so-called residuals are not randomly scattered about zero. The presence of structure in the plots means that the computed line

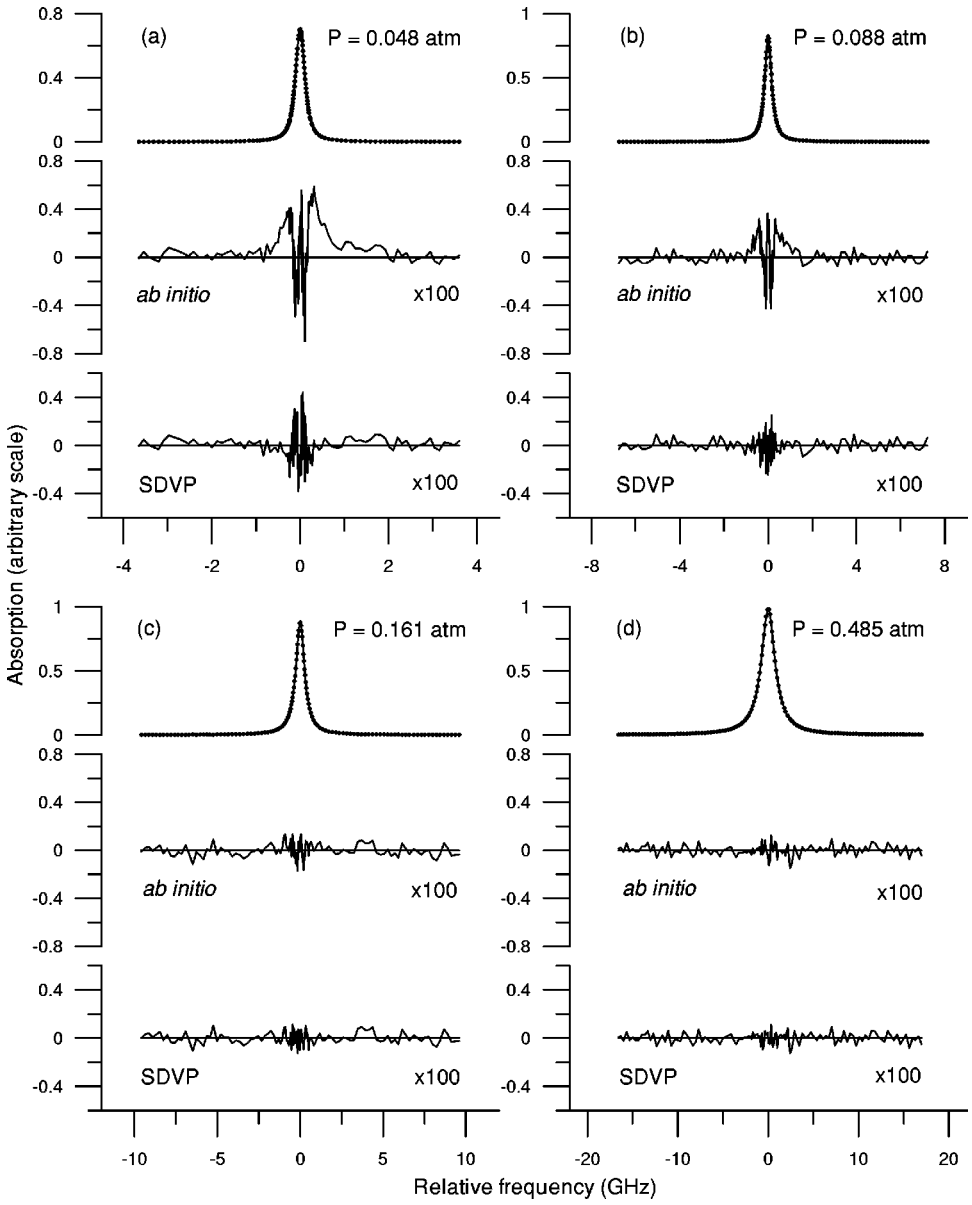

FIG. 2. Plots for four pressures of upper panels: the *ab initio* profile and experimental points, middle panels: residuals or differences between the calculated *ab initio* profile and the measured points, joined by straight line sections, and lower panels: the same as above except that the translational motion was assumed to be collisionless for the calculated profile, a SDVP.

shapes do not agree, in general, with the experimental line shapes. The disagreement is largest at the lowest pressure and decreases with increasing pressure. At 0.485 atm and higher it is difficult, from a visual examination, to see any structure above the noise level, in plots of the residuals. The reader should not be distracted by the changing character of the noise as one moves from low to high pressures. At the lowest pressures the lines are sufficiently narrow that the experimental frequency jitter (± 1.5 MHz) adds to the fluctuations in the absorption. For the two narrowest lines, the fitting routine yields a nonphysical offset in the wings. We have manually adjusted the base line in Figs. 2(a) and 2(b) to produce zero residual in the wings and we have verified that the residuals found by refitting the profiles with this new and fixed base line are indistinguishable (except for the offset) from the original plots. We now discuss possible sources of the discrepancy between the calculated and measured profiles.

IV. DISCUSSION

First we consider the possibility that our choice of rigid spheres (billiard balls) to describe the translational motion is the source of the discrepancy at low pressures. Above we argued that details of the translational motion are insensitive to the choice of potential, provided the potential parameters were chosen to yield the same diffusion constant. Here we provide quantitative support for the argument. Calculations [21,22] show, at least for equal masses, that the translational motion for several potentials, including rigid spheres falls between two extremes, one being the soft collision model of Galatry [23] and the second the so-called hard collision model of Nelkin and Ghatak [24]. Both models have the diffusion constant D as an input parameter. Using the same value of D [18] we have calculated a theoretical, speed-dependent, soft collision profile (SDGP) and a theoretical, speed-dependent, hard collision profile (SDNGP). Plots of the residuals for both profiles have essentially the same

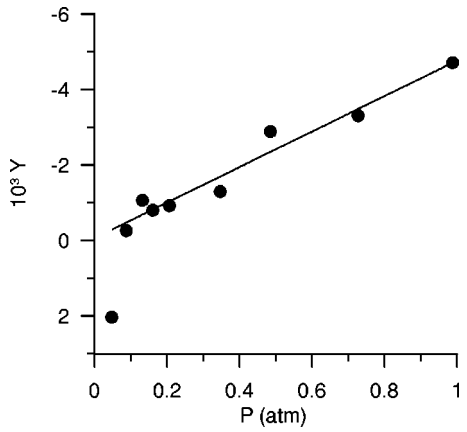

FIG. 3. The weak mixing parameter for $P(2)$ line of CO-Ar as a function of the total pressure. The straight line fit shown ignores the lowest pressure point.

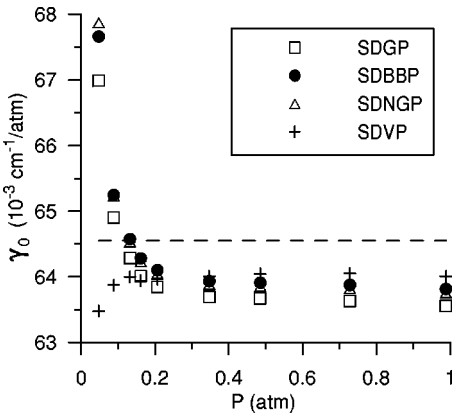

FIG. 4. The fitted values of $\Gamma_0/p=\gamma_0$ as a function of pressure. Filled circles are from the fits to the *ab initio* profile. To illustrate that similar results are found for different models of the translational motion, the figure includes results for the SDGP and the SDNGP. The crosses result when a SDVP is used for the calculated profile. (See text for definition of acronyms.)

structure and size as those shown in Fig. 2 for the low-pressure results. We conclude that the source of the discrepancy is not due to our choice of rigid spheres to describe the translational motion.

In the fitting routine, we allowed for weak mixing by adding a dispersive curve to the profile calculated for an isolated line. Since the calculated and observed curves are very close (remember the scale used to plot the residuals was expanded by a factor of 100 over that used to plot the profiles) it is unimportant that we added it to the calculated profile rather than subtracted it from the experimental profile. Our method avoids the difficulty of determining the asymmetric component for experimental profiles that do not have the points symmetrically recorded about the line center. In Fig. 3 we show as a function of pressure, a plot of the fitted value of the mixing parameter *Y*. There are two signatures present, which convince us that the fitted asymmetries arise from line mixing. The first is that it increases in magnitude in proportion to the pressure. (On close examination, the single anomalous point at the lowest pressure appears to be due to the interplay between the fitting parameters when fitting an incorrect profile to a noisy experimental profile.) The second is the sign, which for the $P(2)$ line is negative. This indicates that the asymmetry is such that the line appears to move towards the ''center of gravity'' of the *P* branch. This is a classic signature of the beginning of the collapse of the branch towards a single line. (Of course, at very high pressures, *P* and *R* branch mixing is expected to collapse the entire rovibrational band to a single line.) Line mixing was measured in CO-CO and CO-N_2 in the first overtone spectrum [25]. There, using an ''energy-corrected sudden approximation,'' they were able to use the measured broadening coefficients to predict the mixing parameters. These compared favorably with the measured asymmetries. Since the broadening in CO-Ar is almost identical to that in CO-CO or CO-N_2, we can from their Fig. 9, predict that the mixing parameter for the $P(2)$ line is close to -5×10^{-3} atm^{-1}. The slope of the line in Fig. 3 is -4.7×10^{-3} atm^{-1}. Clearly, the measured asymmetry can safely be interpreted as arising from line mixing. However, what is much more important is the fact that the correction for line mixing is totally insignificant, on the scale of the plot of the residuals, at the pressures where the disagreement between theory and experiment is large. At 1 atm a value of $Y=-4.7\times10^{-3}$ means that the peak-to-peak mixing correction is 4.7×10^{-3} of the height of the line at line center. At 1 atm this is just twice the peak-to-peak noise in a plot of the residuals. (The noise can always be estimated by looking at a plot of the residuals in the wings of the lines.) In Fig. 2(c) where the discrepancy between the computed and measured profiles is just becoming noticeable, i.e., is above the noise level, the peak-to-peak value of the asymmetry correction is just 0.8×10^{-3} or about 1/3 of the peak-to-peak noise. At lower pressures the correction for line mixing is totally negligible. Clearly, our treatment of the asymmetry cannot be blamed for any disagreement seen in the second panels of Fig. 2.

Next we consider our treatment of the speed-dependent broadening. We have already discussed the case where the PES is known well enough that we can trust the calculated variation of Γ with the speed of the active molecule. What can be questioned is the magnitude of Γ_0 and whether or not it obeys the scaling law $\Gamma_0=\gamma_0 p$, where p is the pressure and γ_0 is a constant, the broadening coefficient. Figure 4 shows a plot of $(\gamma_0)_{fit}=(\Gamma_0)_{fit}/p$ as a function of the pressure. We see at high pressures that the value is constant ($\sim63.9\times10^{-3}$ cm^{-1}/atm) and furthermore that the points lie only 1% below the dashed line, $(\gamma_0)_c=64.55\times10^{-3}$ cm^{-1}/atm, the value calculated directly from the PES, i.e., the two agree within the estimated uncertainty of the calculated value. Note that if the broadening coefficient had been fixed at the calculated value, there would be no agreement between the calculated and the observed line shapes at any pressure. We argue that the close agreement between the calculated and fitted broadening coefficients is not a question of coincidence. We believe that independent of the nature of the velocity changing collisions, correlated or uncorrelated, the maximum *direct* effect the translational motion can have on the width is the pressure-independent

Doppler width, a measure of which is $\omega_D = kv_m$. Thus, at high enough pressures, collisional broadening will always dominate, the width will obey the normal scaling with pressure and the value of γ_0 obtained from the high-pressure fits will be the correct broadening coefficient. For the $P(2)$ line the collisional width equals the calculated Doppler width at 0.048 atm. Our argument amounts to no more than claiming that there exists a collision broadening regime, a commonly held view. We note in passing that the same view was implicitly assumed in Ref. [4] to fit spectra for the value of n appearing above in our expression of $\Gamma(v)$ in terms of a hypergeometric function. (Our n is to be identified with μ in Ref. [4].) In fact it is surprising that the value of $n=0.5$, deduced from the results reported in Ref. [4], is very close to our value of 0.500(6), given that the authors claim that their results are not sensitive to the assumed form for the speed dependence of the broadening. Believing that the high-pressure behavior of $(\gamma_0)_{fit}$ is physically correct, we must conclude that the unphysical behavior of $(\gamma_0)_{fit}$ is the sudden rise with decreasing pressure seen in Fig. 4. If we had demanded that the collisional broadening coefficient was a constant, rather than adjusting it to minimize the residual, then the residuals shown in the middle panels in Figs. 2(a)–2(d) would have been even bigger. Finally, to illustrate again that the broadening results are not very sensitive to the description of the translational motion, we have included in Fig. 4 the values of $(\gamma_0)_{fit}$, which result when we describe the translational motion either by the soft or the hard collision model. The unphysical behavior of $(\gamma_0)_{fit}$ at low pressures is found for all three models for the translational motion.

Having shown that the source of the discrepancy between the calculated and experimental profiles is neither due to our choice of rigid spheres for the translational motion nor due to our calculated speed-dependent broadening, we must conclude that the transport/relaxation equation itself is flawed. Since the only assumption made about the master equation was the lack of statistical correlation, we conclude that the experimental line shape provides evidence for the presence of statistical correlation between the effects of collisions on the translational motion and the effects of collisions on the optical coherence (off-diagonal elements of the density matrix) for the $P(2)$ line in CO-Ar.

There are no *ab initio* calculations of the profile of an isolated line for the correlated case, in spite of the fact that a formal expression of the transport/relaxation equation, in terms of collision kernels, was given some years ago (see Eq. (11) in Ref. [6]). However, Rautian and Sobelmann [2] proposed a mathematical model to account for statistical correlation. The consequence of their model is to reduce the effect of Dicke narrowing. In the extreme case, there would be no narrowing, or equivalently, there would not be a hydrodynamic limit for the translational motion. Consequently the collision dominated regime is to be defined by $\Gamma \gg \omega_D$ rather than by a Dicke width k^2D, less than ω_D. The latter condition, which is often expressed by $z \gg 1$, where z is the narrowing parameter, is appropriate for the uncorrelated case and specifies the hydrodynamic regime. For the $P(2)$ line in CO-Ar, Γ equals ω_D at 0.048 atm, and z equals 1 at 0.128 atm. Consequently, if Dicke narrowing does not occur, our calculations will lead to a width that is too low, for pressures up to ≈ 0.128 atm. The fitting routine, with a nonzero narrowing parameter, would then compensate by increasing the fitted value of the collisional width. The behavior of $(\gamma_0)_{fit}$ shown in Fig. 4 is consistent with this view. This correlation between the broadening and the narrowing has been noted by others when both are fitted parameters (see Ref. [10], and references therein). Logically, the Rautian-Sobelmann model [2] for statistical correlation suggests that the speed-dependent Voigt profile (SDVP) [26] would be a reasonable model for the extreme case of zero Dicke narrowing. Others [27–29] have noted the need to use a zero or reduced narrowing parameter to fit experimental data. In fact, using our calculated expression for $\Gamma(v)$, we find that the SDVP fits the spectra as well or better than the *ab initio* profiles. The residuals for this comparison of theory (model) and experiment are shown in the third panels in Figs. 2(a)–2(d). In addition, the fitted values of the broadening coefficients, shown as crosses in Fig. 4, are better behaved at low pressures than the values resulting from fitting our calculated profiles to the experimental data. However, at the lowest pressures, $(\gamma_0)_{fit}$ falls below the high-pressure asymptotic value, rather than above, and there is a structure in the residual plot at the lowest pressure of 0.048 atm. Thus the SDVP is not the correct spectral profile for the $P(2)$ line of CO heavily diluted in Ar.

V. SUMMARY

In Ref. [4] measurements for each line were made at two pressures, one at low pressure ($\sim 1/10$ atm) and one at high pressure ($\sim 3/4$ atm). Based on an analysis of each line, using a *model for the speed dependence of the broadening* and a variety of *models of the spectral line shape*, the authors concluded that it was plausible for statistical correlation to exist in the CO-Ar system, being severe for low values of J. Here we have *modeled the transport/relaxation equation* itself by assuming uncorrelated motion, but we have solved the equation, using realistic interaction potentials, to obtain *ab initio* spectral profiles of the $P(2)$ line, for a range of pressures. By showing that the computed profiles disagree with the experimental line shapes, we have demonstrated unequivocally that our model transport/relaxation equation is inadequate; or equivalently that statistical correlation is important for the $P(2)$ line of CO highly diluted in Ar. Consequently, an *ab initio* calculation of the spectral profile will require a full numerical solution of the generalized Waldmann-Snyder equation (see Ref. [6], and references therein) or its scalar counterpart [1]. Such computations will automatically include the effects of statistical correlation but they may not reveal its physical origin.

ACKNOWLEDGMENT

We would like to thank the Natural Sciences and Engineering Council of Canada for their support.

[1] A.D. May, Phys. Rev. A **59**, 3495 (1999).
[2] S.G. Rautian and I.I. Sobelman, UsP. Fiz. Nauk **90**, 209 (1966) [Sov. Phys. Usp. **9**, 701 (1967)].
[3] J. Ward, J. Cooper, and E.W. Smith, J. Quant. Spectrosc. Radiat. Transf. **14**, 555 (1974).
[4] P. Duggan, P.M. Sinclair, R. Berman, A.D. May, and J.R. Drummond, J. Mol. Spectrosc. **186**, 90 (1997).
[5] R. Ciuryło, Phys. Rev. A **58**, 1029 (1998).
[6] R. Blackmore, S. Green, and L. Monchik, J. Chem. Phys. **91**, 3846 (1989).
[7] D.A. Shapiro, R. Ciuryło, J.R. Drummond, and A.D. May, Phys. Rev. A **65**, 012501 (2002).
[8] R. Blackmore, J. Chem. Phys. **87**, 791 (1987).
[9] R. Ciuryło, D.A. Shapiro, J.R. Drummond, and A.D. May, Phys. Rev. A **65**, 012502 (2002).
[10] R. Berman, P.M. Sinclair, A.D. May, and J.R. Drummond, J. Mol. Spectrosc. **198**, 283 (1999).
[11] R.R. Toczyłowski and S.M. Cybulski, J. Chem. Phys. **112**, 4604 (2000).
[12] C. Luo, R. Wehr, J.R. Drummond, A.D. May, F. Thibault, J. Boisolles, J.M. Launay, C. Boulet, J.-P. Bouanich, and J.-M. Hartmann, J. Chem. Phys. **115**, 2198 (2001).
[13] F. Thibault, R. Z. Martinez, J. L. Domenech, D. Bermejo, and J.-P. Bouanich, J. Chem. Phys. (to be published).
[14] J. M. Hutson and S. Green, Version 14, Collaborative Computational Project No. 6 (CCP6) of the UK Science and Engineering Research Council, 1994.
[15] D.R. Flower, G. Bourhis, and J.M. Launay, Chem. Phys. **131**, 187 (2000).
[16] M.J. Lindenfeld and B. Shizgal, Chem. Phys. **41**, 81 (1979).
[17] M.J. Lindenfeld, J. Chem. Phys. **73**, 5817 (1980).
[18] T.R. Marrero and E.A. Mason, J. Phys. Chem. Ref. Data **1**, 3 (1972).
[19] P.M. Sinclair, P. Duggan, R. Berman, A.D. May, and J.R. Drummond, J. Mol. Spectrosc. **181**, 41 (1997).
[20] P.W. Rosenkranz, IEEE Trans. Antennas Propag. **23**, 498 (1975).
[21] R.C. Desai, J. Chem. Phys. **44**, 77 (1966).
[22] R.C. Desai and M. Nelkin, Nucl. Sci. Eng. **24**, 142 (1966).
[23] L. Galatry, Phys. Rev. **122**, 1218 (1961).
[24] M. Nelkin and A. Ghatak, Phys. Rev. **135**, A4 (1964).
[25] A. Predoi-Cross, J.P. Bouanich, D.C. Benner, A.D. May, and J.R. Drummond, J. Chem. Phys. **113**, 158 (2000).
[26] P.R. Berman, J. Quant. Spectrosc. Radiat. Transf. **12**, 1331 (1972).
[27] A.S. Pine, J. Quant. Spectrosc. Radiat. Transf. **62**, 397 (1999).
[28] D. Priem, J.M. Colmont, F. Rohart, G. Wlodarczak, and R.R. Gamache, J. Mol. Spectrosc. **204**, 204 (2000); J.F. D'Eu, B. Lemoine, and F. Rohart, *ibid.* **212**, 96 (2002).
[29] R. M. Herman, in *Spectral Line Shapes*, edited by J. Seidel (AIP Press, New York, 2001), Vol. 11, pp. 237; A.S. Pine and J.P. Looney, J. Mol. Spectrosc. **122**, 41 (1987).